

Kinetics of Free-Radical Graft Polymerization of 1-Vinyl-2-pyrrolidone onto Silica

VAN NGUYEN, WAYNE YOSHIDA, JENG-DUNG JOU, YORAM COHEN

Department of Chemical Engineering, University of California at Los Angeles, 5531 Boelter Hall, Los Angeles, California 90095-1592

Received 27 July 2001; accepted 1 October 2001

ABSTRACT: The kinetics of aqueous free-radical graft polymerization of 1-vinyl-2-pyrrolidone onto silica activated with vinyltrimethoxysilane was studied with a mechanistic polymerization model and experimental data for a temperature range of 70–90 °C. The polymerization was initiated with hydrogen peroxide with initial monomer concentrations ranging from 10 to 40 vol %. The kinetic model, which incorporates the hybrid cage–complex initiation mechanism, describes the experimental polymerization data for which the kinetic order, with respect to the monomer concentration, varies from 1 to $\frac{3}{2}$. Surface chain growth occurs by both monomer addition and homopolymer grafting, although the latter contribution to the total polymer graft yield is less significant. Increasing the initial monomer concentration enhances both surface polymer density and average grafted chain length. Increasing reaction temperature, however, produces a denser surface layer of shorter polymer chains. © 2001 John Wiley & Sons, Inc. *J Polym Sci Part A: Polym Chem* 40: 26–42, 2002

Keywords: poly(vinylpyrrolidone) (PVP); 1-vinyl-2-pyrrolidone; silicas; surface modification; vinylsilane; kinetics; free radical; graft polymerization; cage–complex model; polymer grafting

INTRODUCTION

In recent years, there has been a growing interest in the surface modification of inorganic oxide substrates with covalently bonded polymer phases for a variety of practical applications and for fundamental studies of interfacial phenomena. Applications with polymer-modified substrates include filler–polymer control in polymer composites,¹ support packing for liquid and gas chromatography,^{2–7} biocompatible surfaces,⁸ colloid stability,^{9,10} and modified inorganic membranes.^{11–16} Grafted polymers offer unique opportunities to tailor and manipulate interfacial prop-

erties while retaining the basic mechanical strength and geometry of the supporting solid substrate. For example, a substrate can be modified with a polymer, which is completely miscible with the surrounding fluid medium, yet polymer detachment is prevented by the covalent attachment of the polymer chains to the substrate.

Two popular methods for graft polymerization onto inorganic oxide supports are free-radical polymerization^{6,7,9,11,13,15–32} and anionically initiated polymerization.^{2,3,33,34} Previous studies have shown that the free-radical graft polymerization of vinyl monomers is an efficient and controllable method for creating a dense grafted polymer layer.^{11,13,16,17,26,31,34–37} Free-radical graft polymerization typically involves the formation of both free polymer chains (in the solution) and grafted polymer chains (on the substrate). In this approach, sequential monomer addition to the sur-

Correspondence to: Y. Cohen (E-mail: yoram@ucla.edu)

Journal of Polymer Science: Part A: Polymer Chemistry, Vol. 40, 26–42 (2002)
© 2001 John Wiley & Sons, Inc.
DOI 10.1002/pola.10081

face occurs through propagation growth of terminally anchored surface chains (*surface propagation*) and coupling termination reactions between free polymer chains and growing surface chains (*polymer grafting*). In polymer grafting, homopolymer radicals must diffuse toward the solid surface to react with grafted polymer radicals. As a result, diffusion limitations of macromolecules may reduce the contribution of polymer grafting to the overall polymer graft yield. In contrast, in surface propagation, diffusion and steric limitations are diminished because of the smaller size of the monomer molecules.^{11,13,16,17,26,31,34–37}

In this study, the free-radical graft polymerization of 1-vinyl-2-pyrrolidone (VP) onto silica is of particular interest because poly(vinylpyrrolidone) (PVP) is nontoxic and has superior hydrophilic and biocompatible properties.^{8,38,39} Surface-bonded PVP can enhance the performance of size exclusion chromatography resins,⁴ membranes,^{11,13,15,16} and biocompatible hydrogels.³⁸ Studies of VP free-radical graft polymerization onto nonporous silica substrates reported polymer graft yields in excess of 3.5 mg/m², with a number-average molecular weight as high as 20,000 g/mol for the grafted polymer.^{17–19,31} These earlier studies recognized the need for distinguishing the contributions of polymer grafting and surface propagation to the total polymer graft yield. To date, however, a quantitative evaluation of these two competing processes has not been reported. It has also been shown that the free-radical homopolymerization of VP with hydrogen peroxide as an initiator follows an apparent overall polymerization rate order that can reach $\frac{3}{2}$ with respect to the monomer concentration.^{17–19,31,40,61} In earlier studies of the VP system, this kinetic order was incorporated into a kinetic scheme by the empirical setting of the initiation efficiency proportional to the monomer concentration. Although such an empirical model did provide a reasonable fit to experimental monomer conversion data, it did not provide mechanistic insights into the initiation process.

In this study, the free-radical graft polymerization of VP onto vinyltrimethoxysilane (VTMS)-modified silica is analyzed using new and published experimental data with the objective of interpreting the kinetics of the process via a model that incorporates the hybrid cage–complex initiation mechanism.⁴³ It is shown that the proposed mechanistic model can explain the experimentally observed $\frac{3}{2}$ kinetic rate order without resorting to an empirical adjustment of the initi-

ation efficiency. In addition, the behavior of the system is demonstrated via kinetic model simulations of the relative contributions of polymer grafting and surface propagation to the overall polymer graft yield, polymer graft efficiency, molecular weights, and molecular weight distributions of both homopolymers and grafted polymers.

EXPERIMENTAL

The graft polymerization of VP onto silica was carried out via a two-step process previously described by Chaimberg and Cohen.^{17,18} The grafting procedure consisted of the surface activation of silica particles with VTMS, followed by surface polymerization with the VP monomer (Fig. 1). The average surface VTMS concentration and PVP graft yield were determined by thermogravimetric analysis (TGA). The monomer concentration in the solution, and therefore, the conversion of monomer into polymer, were determined via UV spectral analysis.

Materials

Nonporous silica particles (Novacite L207-A), with an average diameter of 5 μm , were obtained from Malvern Minerals Co. (Hot Springs, AK). The silica surface area, measured by Brunauer–Emmett–Teller nitrogen adsorption (Autosorb-1, Quantachrome Corp., Syosset, NY), was approximately 2.2 m²/g. VP monomer, supplied by Aldrich Chemical Co. (Milwaukee, WI), was used as received. VTMS was obtained from Aldrich Chemical. Certified ACS-graded xylene and potassium hydroxide, obtained from Fisher Scientific (Tustin, CA), were used in the silylation process. A 58% aqueous solution of ammonium hydroxide (Mallinckrodt, Inc., Paris, KY) was used as a buffer for the graft polymerization reaction mixture and served as an inhibitor for the formation of undesirable acetaldehyde under acidic conditions. In addition, ammonium hydroxide had a strong activation effect on the polymerization reaction, shortening the latent period and increasing the rate of reaction.^{17,18} Finally, reagent-grade hydrogen peroxide, available as a 30 wt % solution in water (Aldrich Chemical), was used as the initiator.

Silylation

Before the silylation reaction, the silica particles were cleaned with a 1% HCl solution; this was

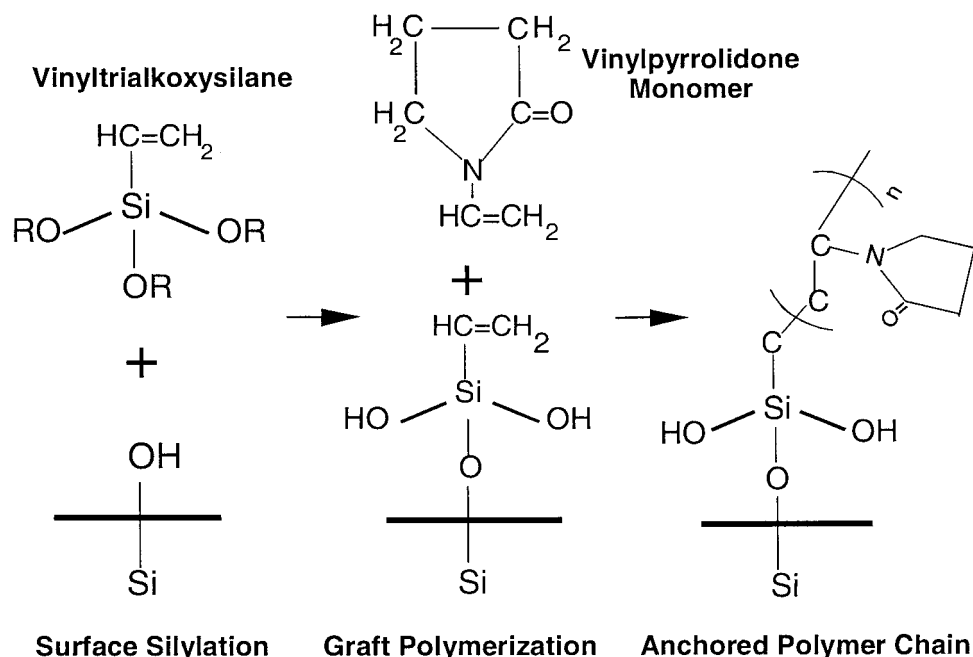


Figure 1. Two-step graft polymerization of VP onto surface-bonded vinyltrialkoxysilane: surface silylation and free-radical graft polymerization.

followed by immersion in water (for hydrolysis of surface siloxanes) and subsequent filtration. The hydroxylated particles were then silylated by an anhydrous solution of 10% VTMS in xylene. The silylation reaction was performed at 137 °C in a slurry batch reactor equipped with a reflux condenser kept at 70 °C, which was above the boiling point of the methanol condensation product yet below the boiling point of the silane solution. The silylated particles were then immersed in an aqueous KOH solution (pH 9.5) to hydrolyze unreacted methoxy groups, thereby partially restoring the hydrophilicity of the surface to improve dispersion of the particles in the aqueous polymerization mixture.⁷ VTMS surface coverage was determined by TGA (TGS-2, PerkinElmer, Norwalk, CT).

Graft Polymerization

The free-radical graft polymerization of VP onto VTMS-modified silica particles, initiated by a mixture of hydrogen peroxide and ammonium hydroxide as a cocatalyst, was carried out in a water-jacketed slurry batch reactor. The reaction mixture was kept under a nitrogen atmosphere, with the reaction temperature controlled to within 0.1 °C by a circulating water bath (Neslab Instruments, Inc., Portsmouth, NH). During the

reaction, 2-mL aliquots of the reaction mixture were withdrawn at various time intervals, and a copious amount of water was added to each sample to quench the reaction. Withdrawn samples were filtered through a 1.0- μm polyester membrane (Nuclepore Corp., Pleasanton, CA) and thoroughly washed with deionized water to remove physically adsorbed monomer and homopolymer. The samples were then dried in a vacuum oven at 110 °C. The polymer graft yield (mg of polymer/g of silica) was determined by measurement of the weight loss upon heating of the polymer-grafted particles from 100 to 700 °C at a rate of 25 °C/min.

The conversion of monomer to polymer was determined by UV spectral analysis (HP 8452A diode array spectrophotometer, Hewlett-Packard, Palo Alto, CA). Calibration curves verified that Beer's law was obeyed for PVP concentrations of up to 8 $\mu\text{g/g}$ at $\lambda = 196 \text{ nm}$ [$\epsilon = 0.13 \text{ (cm } \mu\text{g/g)}^{-1}$] and for VP concentrations of up to 20 $\mu\text{g/g}$ at $\lambda = 233 \text{ nm}$ [$\epsilon = 0.51 \text{ (cm } \mu\text{g/g)}^{-1}$].^{17–19} The carbonyl group, displaying an absorption peak at 196 nm, is found in both the VP monomer and PVP. However, the vinyl group, which reveals an UV absorption peak at 233 nm, only is found in the VP monomer.^{45–48} Therefore, with the carbonyl group as an internal standard, the ratio of absorbances at 233 and 196 nm is related

to the ratio of monomer concentration to polymer concentration in the reaction mixture. Accordingly, the monomer conversion can be calculated from^{17–19}

$$\text{Conversion}_t = 1 - \frac{[\text{M}]_t}{[\text{M}]_{t_0}} = 1 - \left(\frac{A_{233\text{nm}}}{A_{196\text{nm}}} \right)_t \left(\frac{A_{196\text{nm}}}{A_{233\text{nm}}} \right)_{t_0} \quad (1)$$

where subscript t denotes time, $[\text{M}]$ is the monomer concentration, and A is absorbance.

MODEL DEVELOPMENT

It has been well established that the rate of free-radical homopolymerization, for certain vinyl monomers, can have a greater than first-order dependence on the monomer concentration. In particular, two mechanisms have been proposed to account for these high rate orders: the cage-effect theory⁴⁹ and the cage-complex theory.^{50,51} The cage-effect theory assumes that the initiator and solvent molecules can form a cage structure in which the two initiator fragments can recombine several times before diffusing out of the cage.⁴⁹ The cage-complex theory assumes a reversible formation of an association complex between the monomer and initiator pair.^{50,51} This complex decomposes to produce a primary initiator radical and a monomer radical. Noyes⁵² proposed a broader cage-effect model based on a hierarchical cage structure in which primary, secondary, and tertiary recombination between two initiator fragments was introduced. In a later study, Hunkeler⁴³ combined the cage-complex and hierarchical cage mechanisms into a hybrid cage-complex model, which was illustrated for persulfate-initiated acrylamide homopolymerization. In this latter model, the initiator is assumed to exist in a compact-cage structure, in which the two radical fragments are less than one molecular diameter apart, or in a diffuse-cage structure, in which the two radical fragments have diffused further apart. It has been further argued that only the latter structure is susceptible to monomer attack. The monomer-enhanced decomposition competes with the initiator thermal bond rupture in initiating new chain radicals and thus in controlling the overall rate of polymerization.

In this study, the hybrid cage-complex initiation is adopted to account for the observed kinetic

order for the VP system. Monomer-enhanced initiation is feasible in this system, in which hydrogen-bonding association between the VP monomer and hydrogen peroxide as an initiator is possible. Indeed, hydrogen-bonding association between surface-bonded VTMS and hydrogen peroxide should also be possible. However, because of the limited mobility of surface active sites (compared with that of monomer molecules), sensitivity studies for this system have indicated that the kinetic rate coefficient for surface-initiator association is 3 orders of magnitude smaller than the kinetic rate coefficient for monomer-initiator association. Therefore, it is reasonable to neglect the association between the surface VTMS and initiator pair. Furthermore, previous studies on VP homopolymerization with hydrogen peroxide as an initiator have indicated that, for the range of reaction conditions employed in this study, chain-transfer reactions with water, hydrogen peroxide, and terminated polymer molecules are negligible.^{40,53,54} Therefore, only chain-transfer reactions with monomer and surface VTMS are considered in this work. An additional simplification is made in which the long-chain hypothesis (invariance of rate coefficients with respect to chain length) is invoked for propagation, chain-transfer, and termination reactions for both homopolymer and grafted polymer chains.

With these simplifications, the polymerization mechanism for the homopolymer and grafted polymer formation can be described, as given in Table I, by the customary initiation, propagation, chain-transfer, and termination steps. In this reaction scheme, I_2 , (I_2) , and (I_2^*) designate the undissociated, compact-cage, and diffuse-cage initiators, respectively; I^\bullet , M , and S are the initiator radical, monomer, and surface active site, respectively; M_n^\bullet and S_n^\bullet denote the growing homopolymers and grafted polymers, respectively; and H_n and G_n designate the terminated homopolymers and grafted polymers, respectively. The forward and reverse rate coefficients for the compact-cage initiator and diffuse-cage initiator (eq 2) are given by k_1 and k_{-1} and k_2 and k_{-2} , respectively. The reaction rate coefficient for the thermal decomposition of the diffuse-cage initiator is given by k_d (eq 2) with an efficiency of f_d ; the formation and dissociation rate coefficients of the monomer-initiator associate (eqs 3 and 4) are denoted by k_{fimi} and k_{dimi} , respectively, with the efficiency for the monomer-initiator associate dissociation specified by f_{dimi} . The initiation rate coefficients of the free and grafted polymer radicals

Table I. Proposed Reaction Scheme for the Free-Radical Graft Polymerization of VP onto VTMS-Modified Silica with Hydrogen Peroxide as an Initiator

<p>Initiation</p> $\text{I}_2 \xrightleftharpoons[k_{-1}]{k_1} (\text{I}_2) \xrightleftharpoons[k_{-2}]{k_2} (\text{I}_2^*) \xrightarrow{k_3} 2\text{I}\bullet \quad (2)$ $(\text{I}_2^*) + \text{M} \xrightarrow{k_{\text{imi}}} \text{IMI} \quad (3)$ $\text{IMI} \xrightarrow{k_{\text{dmi}}} \text{I}\bullet + \text{M}_1\bullet + \text{H}_2\text{O} \quad (4)$ $\text{I}\bullet + \text{M} \xrightarrow{k_{\text{im}}} \text{M}_1\bullet \quad (5)$ $\text{I}\bullet + \text{S} \xrightarrow{k_{\text{is}}} \text{S}_1\bullet \quad (6)$	<p>Chain Transfer</p> $\text{M}_n\bullet + \text{M} \xrightarrow{k_{\text{trmm}}} \text{H}_n + \text{M}_1\bullet \quad (9)$ $\text{S}_n\bullet + \text{M} \xrightarrow{k_{\text{trsm}}} \text{G}_n + \text{M}_1\bullet \quad (10)$ $\text{M}_n\bullet + \text{S} \xrightarrow{k_{\text{trms}}} \text{H}_n + \text{S}_1\bullet \quad (11)$ $\text{S}_n\bullet + \text{S} \xrightarrow{k_{\text{trss}}} \text{G}_n + \text{S}_1\bullet \quad (12)$
<p>Propagation</p> $\text{M}_n\bullet + \text{M} \xrightarrow{k_{\text{pmm}}} \text{M}_{n+1}\bullet \quad (7)$ $\text{S}_n\bullet + \text{M} \xrightarrow{k_{\text{psm}}} \text{S}_{n+1}\bullet \quad (8)$	<p>Termination</p> $\text{M}_m\bullet + \text{M}_n\bullet \xrightarrow{k_{\text{tmm}}} \text{H}_{m+n} \quad (13)$ $\text{M}_m\bullet + \text{M}_n\bullet \xrightarrow{k_{\text{tdmm}}} \text{H}_m + \text{H}_n \quad (14)$ $\text{S}_m\bullet + \text{M}_n\bullet \xrightarrow{k_{\text{tms}}} \text{G}_{n+m} \quad (15)$ $\text{S}_m\bullet + \text{M}_n\bullet \xrightarrow{k_{\text{tdsm}}} \text{G}_m + \text{H}_n \quad (16)$ $\text{S}_m\bullet + \text{S}_n\bullet \xrightarrow{k_{\text{tss}}} \text{G}_{m+n} \quad (17)$ $\text{S}_m\bullet + \text{S}_n\bullet \xrightarrow{k_{\text{tdss}}} \text{G}_m + \text{G}_n \quad (18)$

by the initiator radical are given by k_{im} and k_{is} (eqs 5 and 6). The homopolymer propagation rate coefficient is given by k_{pmm} (eq 7), and the propagation rate coefficient k_{psm} is for the reaction between a growing grafted polymer and a monomer (eq 8). The rate coefficients for chain-transfer reactions of a growing homopolymer and a growing grafted polymer with a monomer are denoted by k_{trmm} and k_{trsm} , respectively (eqs 9 and 10). Similarly, the reaction rate coefficients for chain-transfer reactions of a growing homopolymer and a growing grafted polymer with a surface site are given by k_{trms} and k_{trss} (eqs 11 and 12). The combination and disproportionation rate coefficients are specified by k_{tmm} and k_{tdmm} for termination reactions between two growing homopolymer chains (eqs 13 and 14), k_{tms} and k_{tdms} are the rate coefficients for termina-

tion reactions between a growing homopolymer chain and a growing grafted chain (eqs 15 and 16), and k_{tss} and k_{tdss} are the rate coefficients for termination reactions between two growing grafted chains (eqs 17 and 18).

The rate expressions for the various species in the reaction mixture are obtained, according to the proposed kinetic mechanism (Table I), with the mass balance equations listed in Table II. In writing the model equations, we have introduced a set of lumped rate coefficients defined as follows: $k_{\text{tmm}} \equiv k_{\text{tmm}} + k_{\text{tdmm}}$, $k_{\text{tms}} \equiv k_{\text{tms}} + k_{\text{tdsm}}$, and $k_{\text{tss}} \equiv k_{\text{tss}} + k_{\text{tdss}}$. The set of kinetic expressions given in Table II form the basis for this kinetic model, which can be further simplified subject to the following approximations:

Table II. Rate Expressions Corresponding to the Proposed Reaction Scheme (Table I)

$$\begin{aligned} \frac{d[I_2]}{dt} &= -k_1[I_2] + k_{-1}[(I_2)] & (19) \\ \frac{d[(I_2)]}{dt} &= k_1[I_2] - k_{-1}[(I_2)] - k_2[(I_2)] + k_{-2}[(I_2^*)] & (20) \\ \frac{d[(I_2^*)]}{dt} &= k_2[(I_2)] - k_{-2}[(I_2^*)] - f_d k_d [(I_2^*)] - k_{fimi}[(I_2^*)][M] & (21) \\ \frac{d[I\bullet]}{dt} &= 2k_d[(I_2^*)] + f_{dimi} k_{dimi} [IMI] - k_{im}[I\bullet][M] - k_{is}[I\bullet][S] & (22) \\ \frac{d[IMI]}{dt} &= k_{fimi}[(I_2^*)][M] - f_{dimi} k_{dimi} [IMI] & (23) \\ \frac{d[M_n\bullet]}{dt} &= f_{dimi} k_{dimi} [IMI] + k_{im}[I\bullet][M] + k_{trsm}[S_n\bullet][M] - k_{trms}[M_n\bullet][S] - 2k_{trmm}[M_n\bullet]^2 - k_{tss}[S_n\bullet][M_n\bullet] & (24) \\ \frac{d[S_n\bullet]}{dt} &= k_{is}[I\bullet][S] - k_{trsm}[S_n\bullet][M] + k_{trms}[M_n\bullet][S] - k_{tss}[S_n\bullet][M_n\bullet] - 2k_{tss}[S_n\bullet]^2 & (25) \\ \frac{d[H_n]}{dt} &= k_{trmm}[M_n\bullet][M] + k_{trms}[M_n\bullet][S] + (k_{tcmm} + 2k_{tdmm})[M_n\bullet]^2 + k_{tdsm}[S_n\bullet][M_n\bullet] & (26) \\ \frac{d[G_n]}{dt} &= k_{trsm}[S_n\bullet][M] + k_{trss}[S_n\bullet][S] + k_{tss}[S_n\bullet][M_n\bullet] + (k_{tcss} + 2k_{tdss})[S_n\bullet]^2 & (27) \\ R_M &= -\frac{d[M]}{dt} = k_{fimi}[(I_2^*)][M] + k_{im}[I\bullet][M] + k_{pmm}[M_n\bullet][M] + k_{psm}[S_n\bullet][M] + k_{trmm}[M_n\bullet][M] + k_{trsm}[S_n\bullet][M] & (28) \\ R_S &= -\frac{d[S]}{dt} = k_{is}[I\bullet][S] + k_{trms}[M_n\bullet][S] + k_{trss}[S_n\bullet][S] & (29) \end{aligned}$$

1. The pseudo-steady-state hypothesis is invoked for intermediate and radical species: IMI, I•, M_n•, and S_n•.
2. The fractions of monomer consumed in the initiation and chain-transfer reactions are negligible compared with that consumed in the propagation step.
3. In this study, as in most typical graft polymerization processes, the initial monomer concentration is significantly higher than the initial surface active site concentration (on a volume basis). Therefore, the growing homopolymer should be more abundant than the growing grafted polymer throughout the grafting process ($[M_n\bullet] \gg [S_n\bullet]$).^{17–19,31}
4. The long-chain hypothesis is invoked for both homopolymer and grafted polymer chains, thereby introducing the following simplifications: $k_{psm} \approx k_{pmm} \equiv k_p$, $k_{trsm} \approx k_{trmm} \equiv k_{trm}$, $k_{trss} \approx k_{trms} \equiv k_{trs}$, $k_{tcsm} \approx k_{tcmm} \equiv k_{tc}$, and $k_{tdss} \approx k_{tdsm} \approx k_{tdmm} \equiv k_{td}$.^{55,56}

The rate expressions for the monomer and surface active site can be simplified, given the above approximations, to yield for the monomer

$$R_M = -\frac{d[M]}{dt} = k_p[M_n\bullet][M] + k_p[S_n\bullet][M] \quad (30)$$

and for the surface active site

$$R_S = -\frac{d[S]}{dt} = k_{is}[I\bullet][S] + k_{trsm}[M_n\bullet][S] \quad (31)$$

The concentrations of radicals and intermediate species, appearing in eqs 22–25, can be expressed by simple algebraic expressions (given the approximations 1–4).

For the monomer–initiator associate,

$$[IMI] = \frac{k'_{fimi}}{f_{dimi} k_{dimi}} [I\bullet][M] \quad (32)$$

For the initiator radical,

$$[I\bullet] = \frac{2k'_d + k'_{fimi}[M]}{k_{im}[M] + k_{is}[S]} [I_2] \quad (33)$$

For the growing homopolymer,

$$[M_n \bullet] = \left(\frac{k'_d + k'_{\text{fimi}}[M]}{k_t} \right)^{1/2} [I_t]^{1/2} \quad (34)$$

For the growing grafted polymer,

$$[S_n \bullet] = \frac{k_{\text{is}}[I \bullet] + k_{\text{trs}}[M_n \bullet]}{k_{\text{trm}}[M] + k_t[M_n \bullet]} [S] \quad (35)$$

in which the total initiator concentration, $[I_t]$, in eqs 32–34 is defined by⁴³

$$[I_t] = [I_2] + [(I_2)] + [(I_2^*)] \quad (36)$$

where $[I_2]$, $[(I_2)]$, and $[(I_2^*)]$ can be expressed as $[I_2] = \varphi_0[I_t]$, $[(I_2)] = \varphi_1[I_t]$, and $[(I_2^*)] = \varphi_2[I_t]$. φ_0 , φ_1 , and φ_2 designate the molar fractions of undissociated, compact-cage, and diffuse-cage initiators, respectively, such that $\varphi_0 + \varphi_1 + \varphi_2 = 1$.⁴³ The kinetic rate equation for the total initiator concentration, obtained from eqs 19–21 and 36, is given by

$$\frac{d[I_t]}{dt} = -(k'_d + k'_{\text{fimi}}[M])[I_t] \quad (37)$$

where the lumped rate coefficients are defined by $k'_d \equiv \varphi_2 f_d k_d$ and $k'_{\text{fimi}} \equiv \varphi_2 k_{\text{fimi}}$.⁴³ We note that the first and second terms in the numerator of eq 33 represent the generation of initiator radicals by thermal bond rupture and monomer-enhanced decomposition of the diffuse-cage initiator, respectively. Similarly, the concentration of growing homopolymer chains is also governed by thermal bond rupture and monomer-enhanced decomposition of the diffuse-cage initiator (eq 34). Finally, the concentration of surface macroradicals is dictated by surface initiation by initiator radicals and growing polymer chains, as represented by the first and second terms in the numerator of eq 35, respectively.

The overall kinetic rate order for homopolymerization can be elucidated by a simplification of eq 30 with the approximation (3) and eq 34. Accordingly, the rate of homopolymerization can be written as

$$R_M = k_p \left(\frac{k'_d + k'_{\text{fimi}}[M]}{k_t} \right)^{1/2} [I_t]^{1/2} [M] \quad (38)$$

When thermal decomposition dominates (i.e., $k'_d \gg k'_{\text{fimi}}[M]$), $[I_t]$ is independent of the monomer concentration (see eq 37), and so the overall rate

of monomer polymerization (eq 38) is linearly proportional to the monomer concentration. When monomer-enhanced decomposition dominates (i.e., $k'_{\text{fimi}}[M] \gg k'_d$), one may observe a $\frac{3}{2}$ overall polymerization order, with respect to the monomer, if the change in $[I_t]$ over the course of the reaction is negligible. The assumption of constant $[I_t]$ was made, either explicitly or implicitly, in previous kinetic studies in which the cage–complex model was used. In the general case, however, when monomer-enhanced initiation is dominant and the variation of $[I_t]$ with the monomer concentration is considered (eq 37), one can deduce, by dividing eq 37 by 38 and integrating the resulting equation, that the total initiator concentration can be expressed as $[I_t] = (\alpha[M]^{1/2} + \beta)^2$, in which $\alpha = (k_t^{1/2}/k_p)(k'_{\text{fimi}})^{1/2}$ and $\beta = [I_0]^{1/2} - \alpha[M_0]^{1/2}$. Accordingly, when $\alpha[M]^{1/2} \gg \beta \geq 0$, the polymerization rate order varies as $[M]^2$, and when $\beta \gg \alpha[M]^{1/2} \geq 0$, the polymerization rate order varies as $[M]^{3/2}$.

Graft Fraction and Polymer Graft Yield

To calculate the molecular weights of homopolymer and grafted polymer, polymer graft yields, and graft efficiency, it is convenient to first define the instantaneous graft fraction (GF) as the probability that when a monomer molecule is consumed it will be incorporated into a grafted chain, rather than into a free chain in solution. The parameter GF is the ratio of the sum of the contribution of surface propagation (eq 8) and polymer grafting (eq 15) to the total rate of monomer polymerized (eq 30):

$$\text{GF} = \frac{k_p[S_n \bullet][M] + \overline{\text{DP}}_h \xi k_t [S_n \bullet][M_n \bullet]}{R_M} \quad (39)$$

where $\overline{\text{DP}}_h$ denotes the instantaneous number-average degree of polymerization for the homopolymer (presented in the subsequent section). We note that the second term of the numerator of eq 39 represents the average number of monomer units added to the surface with each homopolymer radical. Finally, the term $\xi \equiv \frac{k_{\text{tc}}}{k_t}$ can be regarded as the probability that a chain radical will terminate via a combination reaction, rather than in a disproportionation reaction, and $k_t \equiv k_{\text{tc}} + k_{\text{td}}$. The cumulative graft fraction, $\langle \text{GF} \rangle$, obtained over the course of the reaction for the resulting grafted polymer phase is given by

$$\langle \text{GF} \rangle = \frac{\int_0^t (k_p[S_n \bullet][M] + \overline{\text{DP}}_h \xi k_t[S_n \bullet][M_n \bullet]) dt}{[M_0] - [M]} \quad (40)$$

in which the numerator in eq 40 represents the amount of monomer (mol/L) that has been incorporated into the grafted polymer phase, the denominator in eq 40 is the total monomer consumed up to the reaction time t , and $[M_0]$ designates the initial monomer concentration.

The total monomer mass that has been added to the substrate (g of surface-grafted monomer/m² of silica surface) over the course of the reaction is the experimentally measured polymer graft yield $\langle \text{GY} \rangle$. This parameter is related to the cumulative graft fraction (eq 40) by

$$\langle \text{GY} \rangle = \frac{\langle \text{GF} \rangle ([M_0] - [M]) (M_m)}{[\text{sp}] (\varepsilon)} \quad (41)$$

where M_m is the monomer molecular weight, $[\text{sp}]$ is the initial amount of substrate introduced into the reaction mixture (g of silica/L of solution), and ε is the specific area of the substrate (m² of silica surface/g of silica).

The effectiveness of the grafting process can be quantified in terms of the polymer grafting efficiency, $\langle \text{GE} \rangle$, which is defined as the fraction of initial surface sites onto which polymer chains are grafted:

$$\langle \text{GE} \rangle = \frac{\langle \text{GF} \rangle ([M_0] - [M]) / \langle \overline{\text{DP}}_g \rangle}{[S_0]} \quad (42)$$

where $[S_0]$ denotes the initial surface active site concentration (mol/L) and $\langle \overline{\text{DP}}_g \rangle$ is the cumulative number-average degree of polymerization of the grafted polymer (presented in the subsequent section). We note that the surface chain density (number of grafted chains/substrate area) is simply the product of the grafting efficiency and the initial concentration of surface active sites.

Instantaneous and Cumulative Number-Average Degrees of Polymerization

The instantaneous number-average degree of polymerization for the homopolymer ($\overline{\text{DP}}_h$), which is required in eq 39, is the ratio of the net rate at which monomer is added to free chains to the

total rate of formation of all free chains. The net rate at which monomer is incorporated into the homopolymer is $(1 - \text{GF})R_M$, and so $\overline{\text{DP}}_h$ can be written as

$$\overline{\text{DP}}_h = \frac{(1 - \text{GF})R_M}{k_{\text{trm}}[M_n \bullet][M] + k_{\text{trs}}[M_n \bullet][S] + (2 - \xi)k_t[M_n \bullet]^2} \quad (43)$$

The number-average degree of polymerization for the grafted polymer ($\overline{\text{DP}}_g$) can be similarly determined as the net rate of monomer addition per grafted chain. Accordingly, $\overline{\text{DP}}_g$ is given by

$$\overline{\text{DP}}_g = \frac{(\text{GF})R_M}{k_{\text{trm}}[S_n \bullet][M] + k_{\text{trs}}[S_n \bullet][S] + k_t[M_n \bullet][S_n \bullet]} \quad (44)$$

It is evident from eqs 39 and 44 that $\overline{\text{DP}}_g$ is governed by two competing processes: polymer grafting (which depends on $\overline{\text{DP}}_h$) and surface propagation (which is independent of $\overline{\text{DP}}_h$).

The cumulative average degree of graft polymerization, $\langle \overline{\text{DP}}_g \rangle$, can be calculated from

$$\langle \overline{\text{DP}}_g \rangle = \frac{\langle \text{GF} \rangle ([M_0] - [M])}{N_g} \quad (45)$$

where N_g denotes the molar concentration of grafted polymer chains (mol/L) at monomer concentration $[M]$. This parameter can be determined from the following mass balance:

$$\overline{\text{DP}}_g dN_g = -(\text{GF})dM \quad (46)$$

in which the left-hand side of eq 46 designates the average number of surface monomers (mol/L) in an incremental dN_g number of formed grafted chains and the right-hand side of eq 46 represents the incremental number of monomers (mol/L) added to the surface. Equation 46 can be integrated and combined with eq 45 to yield the following expression for $\langle \overline{\text{DP}}_g \rangle$:

$$\langle \overline{\text{DP}}_g \rangle = \frac{\langle \text{GF} \rangle ([M_0] - [M])}{-\int_{[M_0]}^{[M]} \frac{(\text{GF})}{\overline{\text{DP}}_g} dM} = \frac{\langle \text{GF} \rangle ([M_0] - [M])}{\int_0^t \frac{(\text{GF})R_M}{\overline{\text{DP}}_g} dt} \quad (47)$$

where t is the reaction time at which the monomer concentration has reached the value $[M]$. Finally, the cumulative number-average degree of homopolymerization, $\langle \overline{DP}_h \rangle$, can be obtained in an analogous manner, leading to

$$\begin{aligned} \langle \overline{DP}_h \rangle &= \frac{(1 - \langle GF \rangle)([M_0] - [M])}{-\int_{[M_0]}^{[M]} \frac{(1 - GF)}{DP_h} dM} \\ &= \frac{(1 - \langle GF \rangle)([M_0] - [M])}{\int_0^t \frac{(1 - GF)R_M}{DP_h} dt} \quad (48) \end{aligned}$$

Instantaneous Molecular Weight Distributions

The homopolymer chain size distribution is affected by the cross-termination reactions between homopolymer and grafted polymer radicals. However, for systems in which the amount of monomer consumed by the grafting reaction is much smaller than that consumed by the homopolymerization, the homopolymer chain size distribution should reduce to the Flory–Schulz equation.^{57–59} Accordingly, the number fraction of homopolymer molecules containing x monomer units, $n_h^{(x)}$, can be estimated from

$$n_h^{(x)} = (1 - A_h)(1 - p_h)p_h^{x-1} + A_h(x - 1)(1 - p_h)^2 p_h^{x-2} \quad (49)$$

where A_h is the number fraction of terminated homopolymer molecules formed via the combination reaction and p_h is the probability for a growing homopolymer chain to propagate. In the context of the present model, A_h and p_h are given by

$$A_h = \frac{\xi k_t [M_n \bullet]^2}{k_{trm} [M_n \bullet] [M] + k_{trs} [M_n \bullet] [S] + k_t [M_n \bullet]^2} \quad (50)$$

$$p_h = \frac{k_p [M] [M_n \bullet]}{k_p [M_n \bullet] [M] + k_{trm} [M_n \bullet] [M] + k_{trs} [M_n \bullet] [S] + 2k_t [M_n \bullet]^2} \quad (51)$$

For the grafted polymer phase, it is reasonable to assume that the termination rates between two grafted chain radicals are significantly lower than the corresponding cross-termination rates be-

tween a free chain radical and a grafted chain radical. The approximation should be valid for this system because the growing homopolymer is much more abundant and mobile relative to the growing grafted polymer chains. Therefore, we can obtain the number fraction of grafted polymer molecules containing x monomer units, $n_g^{(x)}$, in an analogous manner:

$$n_g^{(x)} = (1 - A_g)(1 - p_g)p_g^{x-1} + A_g(1 - p_h)(1 - p_g) \sum_{y=1}^{x-1} p_h^{y-1} p_g^{x-y-1} \quad (52)$$

in which p_h is given by eq 51. The number fraction of grafted polymer molecules formed via the combination reaction, A_g , and the probability for a growing grafted chain to propagate, p_g , are given by

$$A_g = \frac{\xi k_t [S_n \bullet] [M_n \bullet]}{k_{trm} [S_n \bullet] [M] + k_{trs} [S_n \bullet] [S] + k_t [S_n \bullet] [M_n \bullet]} \quad (53)$$

$$p_g = \frac{k_p [S_n \bullet] [M]}{k_p [S_n \bullet] [M] + k_{trm} [S_n \bullet] [M] + k_{trs} [S_n \bullet] [S] + k_t [S_n \bullet] [M_n \bullet]} \quad (54)$$

Numerical Analysis

The key parameters in this model are k'_d , k'_{fimi} , k_p , k_{trm} , k_{trs} , k_t , (k_{is}/k_{im}) , and ξ . In this work, the propagation (k_p) and termination (k_t) rate coefficients were obtained from the experimental study of Agasandyan et al.⁶⁰ The rate coefficient for chain transfer with monomer (k_{trm}) and the probability of termination by coupling (ξ) were evaluated by Chaimberg and Cohen^{17,18} on the basis of experimental homopolymer molecular weight data for the VP/hydrogen peroxide system. The apparent rate coefficients for thermal bond rupture (k'_d) and monomer association (k'_{fimi}) were calculated by eqs 37 and 38 fitting to the experimental monomer conversion data. Kinetic parameters involved in surface initiation, k_{is}/k_{im} and k_{trs} , were obtained by the fitting of the model (eqs 37–41 and 43) to the experimental polymer graft yield data. At each given temperature, the fitting was performed with the simplex optimization method (Scientist software, Micromath Inc., UT)

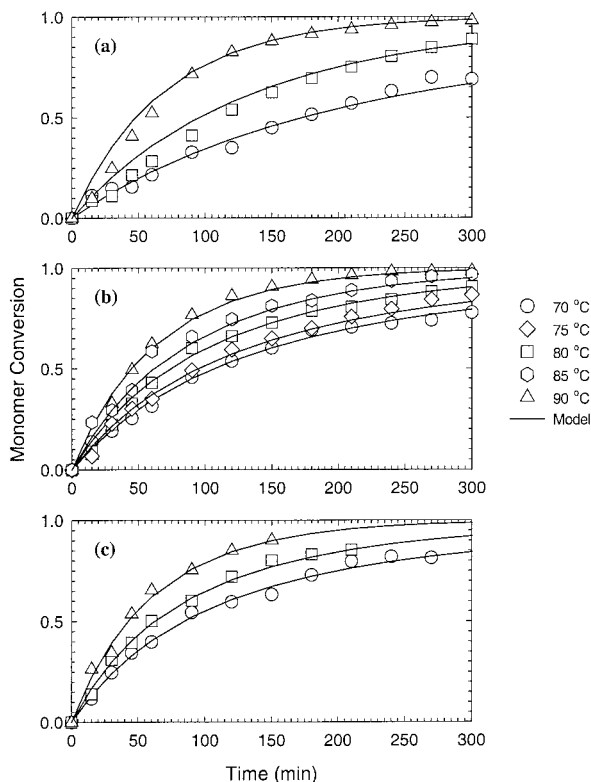


Figure 2. Experimental and model-calculated monomer conversions for vinyl pyrrolidone polymerization: (a) $[M_0] = 0.936M$ and $S_a = 15 \mu\text{mol}$ of vinylsilane/ m^2 of surface, (b) $[M_0] = 2.81M$ and $S_a = 31 \mu\text{mol}$ of vinylsilane/ m^2 of surface, and (c) $[M_0] = 4.68M$ and $S_a = 46 \mu\text{mol}$ of vinylsilane/ m^2 of surface. All data are for $[I_0] = 0.043M$.

with all the available experimental data at various initial monomer, initiator, and surface concentrations.

RESULTS AND DISCUSSION

Monomer Conversion

The kinetic model provides excellent fits to the experimental monomer conversion data, as shown in Figure 2. The increasing rate of monomer conversion with increasing temperature and initial monomer concentration is consistent with previous studies on aqueous VP homopolymerization with hydrogen peroxide as an initiator.^{40,61} For this system, model calculations revealed that, for the range of reaction conditions used, the total initiator concentration decreases by less than 1% over the course of the reaction, with the maximum ratio $k'_{\text{fimi}}[M]/k'_d$

(see eq 38) being as high as 35. Accordingly, under the reaction conditions of this study, the apparent kinetic order of polymerization (see eq 38), with respect to the monomer concentration, ranges from unity at a temperature above about 80 °C and approaches $\frac{3}{2}$ at lower temperatures and low conversions. For the latter regime, new polymer chains are initiated primarily by monomer-enhanced dissociation. However, as monomer concentration decreases and reaction temperature rises, initiation is dominated by thermal bond rupture, and the kinetic rate order approaches unity. Clearly, the excellent fits to the experimental data (over a wide range of conditions) suggest that the proposed initiation mechanism provides an adequate description of the polymerization kinetics without resorting to an empirical adjustment of the initiation efficiency as in previous studies.^{17–19,31,40–42}

The temperature dependence of the homopolymerization rate coefficients obtained from previous studies (i.e., k_p , k_t , k_{trm} , and ξ) along with those extracted in this work (i.e., k'_d , k'_{fimi} , $k_{\text{is}}/k_{\text{im}}$, and k_{trs}) is illustrated in Table III. The rate coefficients for propagation (k_p), chain transfer with monomer (k_{trm}), and termination (k_t) increase with temperature according to an Arrhenius dependence, with k_t being about 4 orders of magnitude larger than k_p . The rate coefficient for thermal bond rupture (k'_d) also increases with temperature according to the Arrhenius relationship, whereas that for monomer association (k'_{fimi}) decreases exponentially over the temperature range of 70–90 °C. The aforementioned temperature-dependent trends can be rationalized by the realization that at a higher reaction temperature, the thermal energy possessed by fragments of the diffuse-cage initiator will increase, producing a higher displacement frequency away from their equilibrium bond distance. This increasing displacement frequency along with a higher concentration of the diffuse-cage initiator φ_2 will result in a higher apparent rate coefficient for the thermal bond rupture.⁴³ However, the apparent rate coefficient for monomer association will decrease with rising reaction temperature despite the rising concentration of the diffuse-cage initiator, which is apparently insufficient to reverse the temperature-dependent trend.

Polymer Graft Yield

The experimental polymer graft yield (mg of surface monomer/ m^2 of silica surface) is reasonably

Table III. Reaction Rate Coefficients for the Free-Radical Graft Polymerization of VP onto VTMS-Modified Silica with Hydrogen Peroxide as an Initiator

Rate Coefficient ^a			
$\ln k = \frac{E}{T} + A$	E (K)	A	Reference
k'_d	-2.033×10^4	46.72	This work
k'_{fmi}	5.7775×10^3	-27.39	This work
k_p	-3.575×10^3	23.14	Agasandyan et al. ⁶⁰
k_{trm}	-3.575×10^3	17.84	Agasandyan et al. ⁶⁰
k_{trs}	-5.647×10^3	23.01	This work
k_t	-8.057×10^2	24.82	Chaimberg and Cohen ³¹
k_{tc}	-8.057×10^2	24.125	Chaimberg and Cohen ³¹
Rate Coefficient Ratio ^a			
$k_{\text{is}}/k_{\text{im}} = BT + C$	B (K ⁻¹)	C	Reference
$k_{\text{is}}/k_{\text{im}}$	-2.034×10^{-2}	7.379	This work

^a Except for k'_d , which is in min^{-1} , all rate coefficients are in L/mol min .

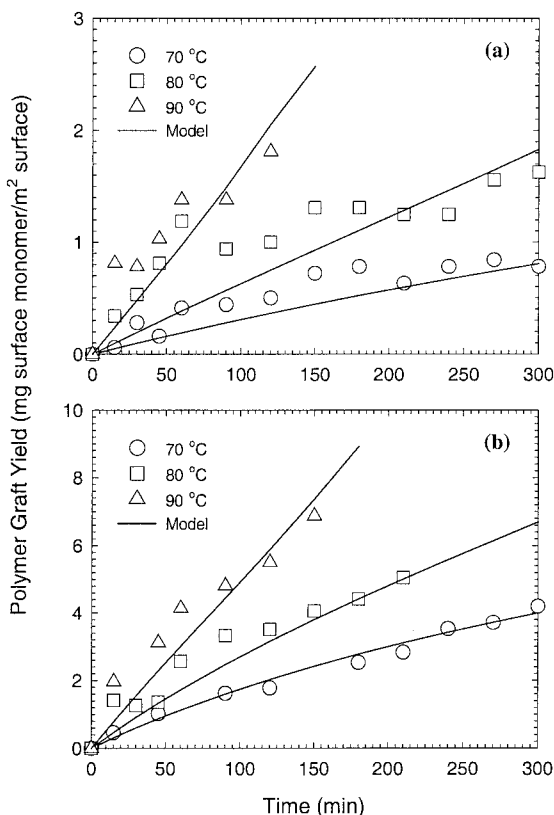


Figure 3. Experimental and model-calculated graft yield data: (a) $[M_0] = 0.936M$ and $S_a = 15 \mu\text{mol}$ of vinylsilane/ m^2 of surface and (b) $[M_0] = 4.68M$ and $S_a = 46 \mu\text{mol}$ of vinylsilane/ m^2 of surface. All data are from $[I_0] = 0.043M$.

well described by the kinetic model, as illustrated in Figure 3. The polymer graft yield increases with both temperature and initial monomer concentration in agreement with a higher rate of monomer polymerized. The scatter in the experimental data is largely due to the sensitivity limit of the thermogravimetric analysis at this low level of polymer graft yield.

The temperature dependence of the extracted rate coefficient ratio ($k_{\text{is}}/k_{\text{im}}$) and the rate coefficient for surface chain transfer (k_{trs}) are given in Table III. $k_{\text{is}}/k_{\text{im}}$ decreases with temperature in accordance with a greater increase of monomer mobility relative to the surface VTMS (i.e., a faster rise in k_{im} compared with k_{is}). The rise of the rate coefficient for surface chain transfer (k_{trs}) with temperature is consistent with the increasing mobility of polymer radicals. Furthermore, the rate coefficient for surface chain transfer (k_{trs}) is smaller (by a factor of 2) than the rate coefficient for chain transfer with monomer (k_{trm}), also consistent with the expected lower mobility of surface active sites.

Species Concentrations

To elucidate the significance of various species in the reaction mixture, their relative concentrations are illustrated in Figures 4 and 5 for a reaction time of 150 min, initial monomer and initiator (hydrogen peroxide) concentrations of 4.61 and 0.043M, and a surface VTMS concentration of 31 $\mu\text{mol}/\text{m}^2$. The monomer concentration,

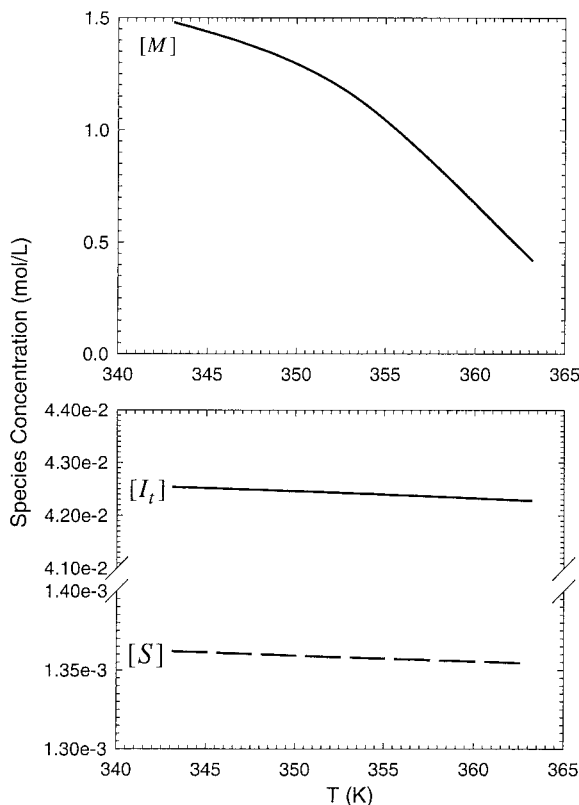


Figure 4. Calculated concentrations of VP monomer ($[M]$), surface-bonded VTMS ($[S]$), and total initiator ($[I_t]$). Data are at the 150-min reaction time, with initial monomer, VTMS, and initiator concentrations of $[M_0] = 4.68M$, $S_a = 31 \mu\text{mol}$ of vinylsilane/ m^2 of surface, and $[I_0] = 0.043M$, respectively.

which is about 3 orders of magnitude higher than the concentration of surface-bonded VTMS (on a volume basis), decreases significantly with rising temperature. In contrast, the total initiator concentration decreases slightly with temperature. A similar trend is also observed for the concentration of surface-bonded VTMS.

The concentrations of polymer species (M_n^\bullet , S_n^\bullet , H_n , and G_n) increase with temperature, which is consistent with a higher rate of monomer consumption due to the formation of both homopolymer and grafted polymer. In addition, the concentration of growing homopolymer in solution (Fig. 5) is about 3 orders of magnitude higher than the concentration of growing grafted polymer. This trend is expected because of the relatively low initial concentration of surface VTMS (on a volume basis). Correspondingly, the concentration of terminated homopolymer is also about 3 orders of magnitude higher than the concentration of terminated grafted polymer.

Instantaneous Number-Average Degrees of Polymerization and Molecular-Weight Distributions

The temperature dependence of the instantaneous number-average degree of graft polymerization (\overline{DP}_g) and the ratio of degrees of homopolymerization to graft polymerization ($\overline{DP}_h/\overline{DP}_g$) are illustrated in Figure 6. As evident from this example, the degree of polymerization for the grafted polymer decreases sharply at a higher temperature. As the temperature increases, the rates of surface chain termination and chain transfer increase more significantly than the increase in the rate of surface chain propagation (Figs. 4 and 5), thereby resulting in a decreasing grafted polymer molecular weight. However, although the rates of both surface chain termination and chain transfer increase with initial monomer concentration, they increase at relatively slower rates compared with the rate of sur-

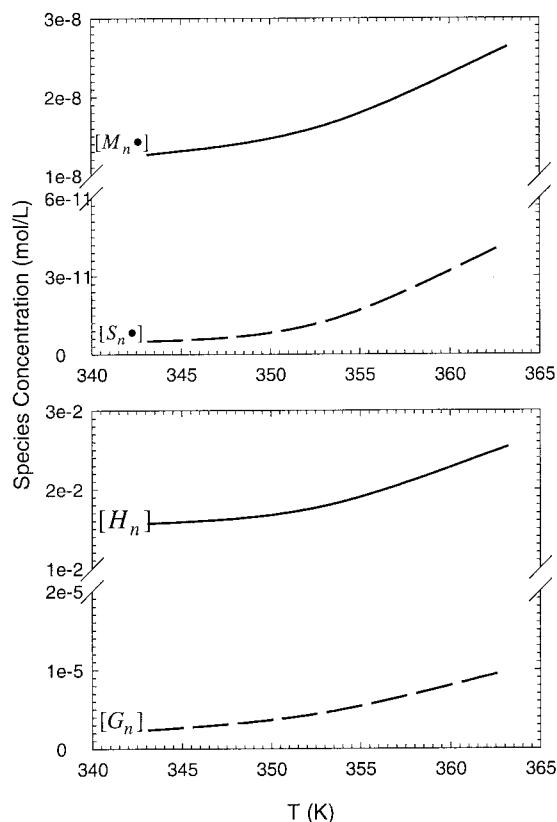


Figure 5. Calculated concentrations for the growing homopolymer ($[M_n^\bullet]$), growing grafted polymer ($[S_n^\bullet]$), terminated homopolymer ($[H_n]$), and terminated grafted polymer ($[G_n]$). Results are for the conditions given in Figure 4.

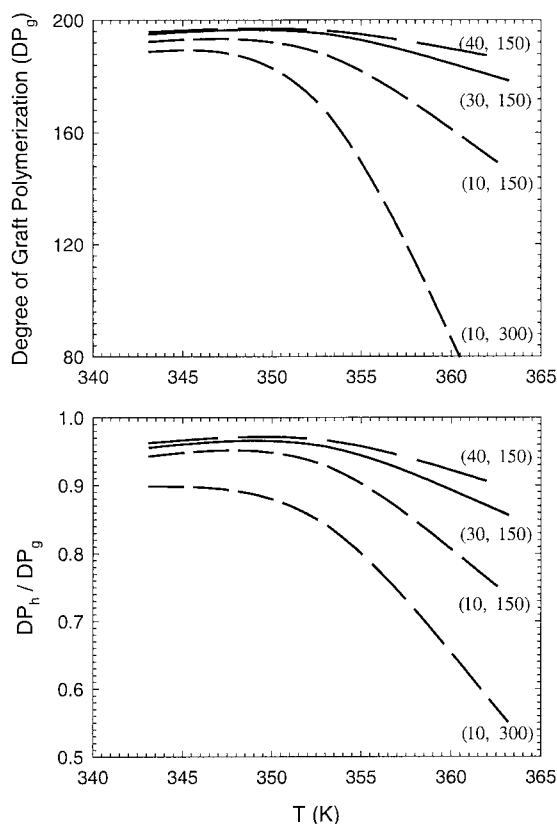


Figure 6. Calculated instantaneous number-average degrees of graft polymerization (\overline{DP}_g) and molecular-weight ratios between the homopolymers and grafted polymers ($\overline{DP}_g/\overline{DP}_h$). The first and second numbers in parentheses denote the initial monomer concentration (vol %) and reaction time (min), respectively. The initial surface density and initiator concentration are $S_a = 31 \mu\text{mol}$ of vinylsilane/ m^2 of surface and $[I_0] = 0.043M$.

face propagation (Figs. 4 and 5). A higher monomer concentration (at a given temperature) provides a net enhancement of the rate of monomer addition to the grafted polymer phase, leading to a longer average grafted chain length. With increasing conversion, however, the molecular weight of the grafted polymer decreases because of bimolecular termination between polymer radicals.

The homopolymer molecular weight decreases with temperature and/or conversion and also increases with initial monomer concentration. Although monomer consumption occurs primarily because of homopolymer propagation (given the low concentrations of surface-bonded VTMS and hydrogen peroxide as an initiator), the rates of chain transfer and termination associated with

the homopolymer are also significantly higher than those associated with the grafted polymer. Conceivably, depending on the reaction conditions and relative magnitude of the reaction rate coefficients, the homopolymer molecular weight can be smaller or larger than the grafted polymer molecular weight. For this VP/silica/hydrogen peroxide system, for example, the homopolymer molecular weight is about 3–45% lower than that of the grafted polymer.

The size distributions of the homopolymers and grafted polymers are similar, as illustrated in Figure 7 at a temperature of 80°C with the initial VP monomer, surface VTMS, and hydrogen peroxide initiator concentrations of $4.68M$, $31 \mu\text{mol}/\text{m}^2$, and $0.043M$, respectively. The polydispersity indices are about 1.94 and 2 for the homopolymer and grafted polymer, respectively. Because the propagation probability for a homopolymer radical (eq 51) is slightly smaller than the corresponding probability for a grafted polymer radical (eq 54), the size distribution of the grafted polymer should be slightly broader. However, because of the significantly lower homopolymer radical concentration, relative to the monomer (Figs. 4 and 5), the distinction between the two distributions for this system is insignificant (although the dif-

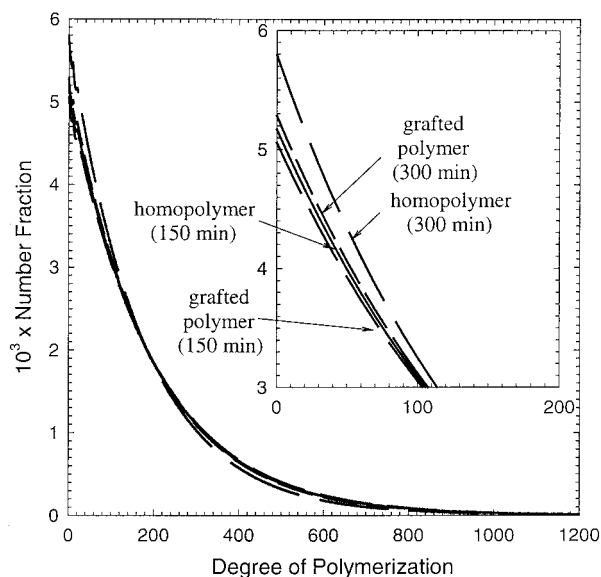


Figure 7. Calculated instantaneous molecular weight distributions at 80°C and for reaction times of 150 and 300 min. The initial VP monomer, surface-bonded VTMS, and hydrogen peroxide initiator concentrations are $[M_0] = 2.81M$, $S_a = 31 \mu\text{mol}$ of vinylsilane/ m^2 of surface, and $[I_0] = 0.043M$, respectively.

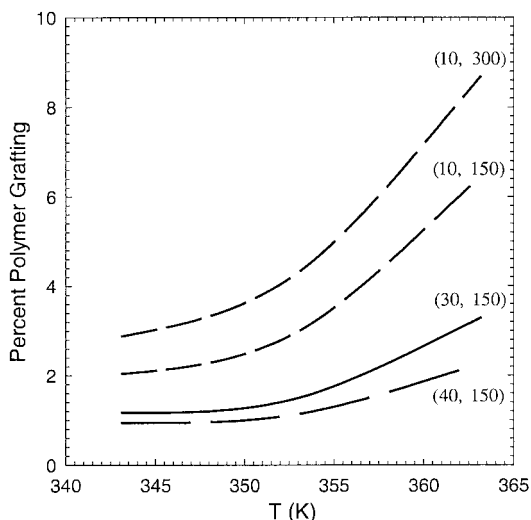


Figure 8. Contributions of polymer grafting (%) to the overall graft yield. Data are for the conditions given in Figure 6.

ference is somewhat more visible at a higher conversion).

Percentage of Polymer Grafting

Practical applications in which a tethered polymer phase is prepared by the present graft polymerization method require a priori estimation of the contribution of polymer grafting (relative to surface propagation) to the overall graft yield. Such information is crucial to better control of the resulting surface chain size distribution and density.^{5,6,19} As an illustration, the calculated percent contributions of polymer grafting for three different initial monomer concentrations are plotted in Figure 8. The contribution of polymer grafting increases with temperature because the concentration ratio of homopolymer radical to monomer increases significantly with increasing temperature, as evident in Figures 4 and 5. The same argument holds with respect to monomer conversion. The relatively lower monomer concentration, combined with the increase in the concentration of polymer radicals at higher conversions, should increase the contribution of polymer grafting to the overall graft yield. Ultimately, surface chain propagation is still the dominant process for surface chain growth. However, its contribution, relative to polymer grafting, declines with rising reaction temperature. In addition, because the rate of chain propagation increases more rap-

idly with monomer concentration, the percent contribution from polymer grafting decreases with initial monomer concentration.

Graft Efficiency

The graft efficiency, defined as the fraction of initial surface active sites onto which polymer chains are grafted, is directly proportional to surface chain density. As illustrated in Figure 9, the graft efficiency increases significantly with temperature and/or monomer conversion and to a lesser extent with rising initial monomer concentration. The potential of activating new surface sites by free polymer radicals will increase as these radicals become more abundant in the reaction mixture and as the reaction temperature increases. Although at higher temperatures more monomer molecules are added to the grafted polymer phase, they are distributed among a larger number of surface chains, thereby producing a denser grafted layer of shorter chains. With respect to the monomer conversion, similar observations also hold regarding the density and molecular weight of the grafted polymer because the polymer radicals become more abundant at a higher conversion. This notwithstanding, the fraction of initial surface sites onto which polymer chains are grafted remains small ($<1.2\%$), suggesting the possibility of shielding of reactive surface sites.

At a higher initial monomer concentration, more monomer molecules are incorporated into

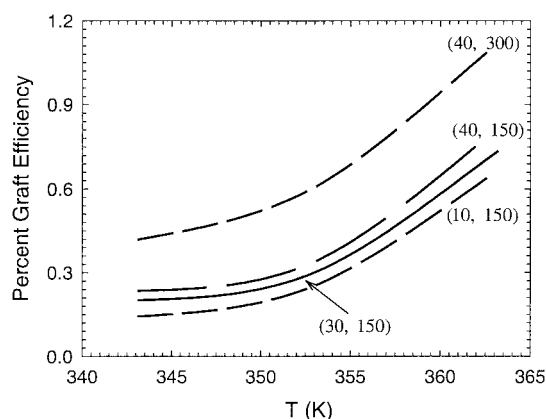


Figure 9. Calculated graft efficiencies. Results are for the conditions given in Figure 6. The first and second numbers in parentheses denote the initial monomer concentration (vol %) and reaction time (min), respectively.

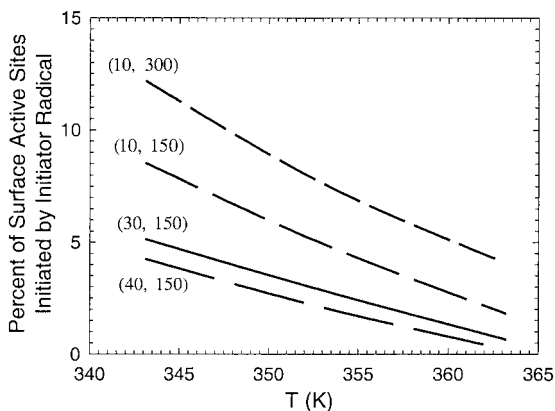


Figure 10. Calculated percentage of surface initiation by the initiator radical. Results are for the conditions given in Figure 6. The first and second numbers in parentheses denote the initial monomer concentration (vol %) and reaction time (min), respectively.

the grafted phase (a higher polymer graft yield), enhancing both the grafted chain length (Fig. 6) and surface chain density (Fig. 9). However, the increase in the number of surface chains is rather modest. At a higher initial monomer concentration, increasing radical scavenging by monomer molecules reduces the number of initiator free radicals available for initiating new surface chains. In other words, if the initiator radicals were the primary mean of surface initiation, surface chain density would decline with initial monomer concentration. However, since the number of homopolymer radicals increases considerably with initial monomer concentration, an initiation process dominated by growing homopolymer would produce a higher surface chain density for a higher initial monomer concentration. Because these two opposing mechanisms are concurrent, they reduce the observed impact of the initial monomer concentration on the graft efficiency. Indeed, for the particular system studied, more than 87% of the surface chains are initiated by the homopolymer radicals (Fig. 10), resulting in a slight increase in polymer graft efficiency with initial monomer concentration.

Finally, although the efficiency of PVP grafting as obtained in this work is seemingly low, if the distance between neighboring anchored chains is smaller than their radius of gyration, the grafted polymer chains will extend away from the surface to maximize their entropy in a conformation analogous to the bristles of a

brush.^{13,16–19,31,32} This situation would lead to a so-called dense brush regime when the following criterion (which assumes a uniform segment distribution) is met⁶²:

$$\sigma = \left(\frac{a}{D}\right)^2 > (\overline{DP}_g)^{-6/5} \quad (55)$$

in which σ is the fractional surface coverage of the grafted polymer, a is the size of a monomer unit, and D is the distance between two neighboring anchoring points on the surface. D between two neighboring chains can be calculated from the graft efficiency ($\langle GE \rangle$) and initial surface active site density (S_a) as follows^{13,16,19}:

$$D = (\langle GE \rangle S_a N_A)^{-1/2} \quad (56)$$

where N_A denotes Avogadro's number. Equation 56 is based on the approximation of evenly spaced square grids of anchoring sites on a flat surface. It can be easily verified that, with a size of 6.4 Å for a VP monomer unit, calculated with the Spartan molecular modeling program (Spartan 4.1, WaveFunction, Inc., CA), eq 55 is satisfied for all the grafting conditions employed in this work (i.e., for the 150-min reaction time, D ranges from 21 to 88 Å, and \overline{DP}_g ranges from 147 to 196), indicating the achievement of a dense brush regime of the grafted polymer phase.^{13,16,19}

CONCLUSIONS

The aqueous free-radical graft polymerization of 2-vinyl-1-pyrrolidone onto nonporous silica has been investigated. The proposed kinetic model, which incorporates the hybrid cage–complex initiation model, describes the experimental polymerization data, which reveal an overall polymerization kinetic order ranging from 1 to about $\frac{3}{2}$ with respect to the monomer concentration. The grafting of chains onto the substrate is attributed to both polymer grafting and surface chain propagation. Kinetic model simulations suggest that the contribution of polymer grafting to the total polymer graft yield is more important at high reaction temperatures and/or low monomer concentrations. Ultimately, however, surface chain propagation is the dominant grafting process. Calculations of the polymer graft efficiency and molecular weight have demonstrated that a

higher reaction temperature promotes the formation of a denser layer of shorter grafted chains, whereas a higher initial monomer concentration enhances both graft density and average grafted chain length.

This work was funded in part by the National Science Foundation, the Electric Power Research Institute, the University of California Toxic Substances Research and Teaching Program, the U.S. Department of Energy, and the University of California at Los Angeles Academic Senate.

REFERENCES AND NOTES

1. Yablokova, N. V.; Aleksandrova, Y. A.; Titova, O. M. *Polym Sci USSR* 1986, 28, 2122.
2. Papirer, E.; Nguyen, V. T. *Polym Lett* 1972, 10, 167.
3. Papirer, E.; Nguyen, V. T. *Angew Makromol Chem* 1973, 128, 31.
4. Krasilnikov, I.; Borisova, V. *J Chromatogr* 1988, 446, 211.
5. Cohen, Y.; Eisenberg, P.; Chaimberg, M. *J Colloid Interface Sci* 1992, 21, 579.
6. Cohen, Y.; Faibish, R. S.; Rovira-Brau, M. In *Interfacial Phenomena in Chromatography*; Pefferkorn, E., Ed.; Marcel Dekker: New York, 1999.
7. Montse, R.-B.; Giralt, F.; Cohen, Y. *J Colloid Interface Sci* 2001, 235, 70.
8. Cohn, D.; Hoffman, A. S.; Ratner, B. D. *J Appl Polym Sci* 1984, 29, 2645.
9. Laible, R.; Hamann, K. *Adv Colloid Interface Sci* 1980, 13, 63.
10. Iwata, H.; Odate, M.; Uyama, Y.; Memiya, H.; Ikada, Y. *J Membr Sci* 1991, 55, 119.
11. Castro, R. P.; Cohen, Y.; Monbouquette, H. G. *J Membr Sci* 1993, 84, 151.
12. Yamaguchi, T.; Yamahara, S.; Nakao, S.; Kimura, S. *J Membr Sci* 1994, 95, 39.
13. Castro, R. P.; Cohen, Y.; Monbouquette, H. G. *J Membr Sci* 1996, 115, 179.
14. Yamaguchi, T.; Miyazaki, Y.; Nakao, S.; Tsuru, T.; Kimura, S. *Ind Eng Chem Res* 1998, 37, 177.
15. Jou, J. D.; Yoshida, W.; Cohen, Y. *J Membr Sci* 1999, 162, 269.
16. Castro, R. P.; Cohen, Y.; Monbouquette, H. G. *J Membr Sci* 2000, 179, 207.
17. Chaimberg, M. Ph.D. Thesis, University of California, Los Angeles, CA, 1989.
18. Chaimberg, M.; Cohen, Y. *Ind Eng Chem Res* 1991, 30, 2534.
19. Jou, J. D. Ph.D. Thesis, University of California, Los Angeles, CA, 1998.
20. Wheals, B. B. *J Chromatogr* 1975, 107, 402.
21. Monrabal, B. *Adv Chromatogr* 1979, 14, 117.
22. Monrabal, B. *Chromatogr Sci* 1981, 19, 79.
23. Parnas, R. S.; Chaimberg, M.; Taepaisitphongse, V.; Cohen, Y. *J Colloid Interface Sci* 1989, 129, 441.
24. Boven, G.; Oosterling, M. L.; Challa, G.; Schouten, A. *Polymer* 1990, 31, 2377.
25. Boven, G.; Folkersma, R.; Challa, G.; Schouten, A. *Polym Commun* 1991, 32, 51.
26. Cohen, Y. U.S. Patent 5,035,803, 1991.
27. Browne, T.; Chaimberg, M.; Cohen, Y. *J Appl Polym Sci* 1992, 44, 671.
28. Carlier, E.; Guyot, A.; Revillon, A.; Darricades, M.; Petiaud, R. *React Polym* 1992, 16, 115.
29. Tsubokawa, N.; Ishida, H. *J Polym Sci Part A: Polym Chem* 1992, 30, 2241.
30. Tsubokawa, N.; Kimoto, T.; Koyama, T. *J Colloid Polym Sci* 1993, 271, 940.
31. Chaimberg, M.; Cohen, Y. *AIChE J* 1994, 40, 294.
32. Castro, R. P. Ph.D. Thesis, University of California, Los Angeles, CA, 1997.
33. Horn, J.; Hoene, R.; Hamann, K. *Makromol Chem Suppl* 1975, 1, 329.
34. Tsubokawa, N.; Kogure, A.; Sone, Y. *J Polym Sci Part A: Polym Chem* 1990, 28, 1923.
35. Ching, C. M.S. Thesis, University of California, Los Angeles, CA, 1992.
36. Ying, H. M.S. Thesis, University of California, Los Angeles, CA, 1995.
37. Bei, N. M.S. Thesis, University of California, Los Angeles, CA, 1999.
38. Hefferman, J. G.; Sherrington, D. C. *J Appl Polym Sci* 1984, 29, 3013.
39. Inoue, H.; Kohama, S. *J Appl Polym Sci* 1984, 29, 877.
40. Woodhams, R. T. Ph.D. Thesis, Polytechnic Institute of Brooklyn, Brooklyn, NY, 1954.
41. Biesenberger, J. A.; Sebastian, D. H. *Principle of Polymerization Engineering*; Wiley-Interscience: New York, 1983.
42. Billmeyer, F. W. *Textbook of Polymer Science*, 3rd ed.; Wiley-Interscience: New York, 1984.
43. Hunkeler, D. *Macromolecules* 1991, 24, 2160.
44. Zubakova, L. B.; Borisova, V. N.; Koroleva, S. K.; Davydov, V. Ya.; Filatova, G. N. *Zh Prik Khim* 1987, 60, 1491.
45. Sundardi, F.; Kadariah, R.; Marlianti, I. *J Appl Polym Sci* 1983, 28, 3123.
46. Oster, G.; Immergut, E. H. *J Am Chem Soc* 1954, 76, 1393.
47. Senogles, E.; Thomas, R. *J Polym Sci Polym Symp* 1975, 49, 203.
48. Senogles, E.; Thomas, R. *J Polym Sci Polym Symp* 1976, 55, 241.
49. Matheson, M. S. *J Chem Phys* 1945, 13, 584.

50. Gee, G.; Rideal, E. K. *Trans Faraday Soc* 1936, 32, 666.
51. Gee, G.; Cuthbertson, A. C.; Rideal, E. K. *Proc R Soc London Ser A* 1939, 170, 300.
52. Noyes, R. M. *J Am Chem Soc* 1955, 77, 2042.
53. Karaputadze, T. M.; Shumskii, V. I.; Kirsh, Yu. E. *Vysokomol Soyed Ser A* 1978, 20, 1854.
54. Shtamm, E. V.; Karaputadze, T. M.; Kirsh, Yu. E. *Zh Fiz Khim* 1981, 55, 2289.
55. Brydon, A.; Burnett, G. M.; Cameron, G. G. *J Polym Sci Polym Chem Ed* 1974, 12, 1011.
56. Huang, N.-J.; Sundberg, D. C. *J Polym Sci Part A: Polym Chem* 1995, 33, 2533.
57. Rosen, S. L. *Fundamental Principles of Polymeric Materials*, 2nd ed.; Wiley-Interscience: New York, 1993; Chapter 10, pp 159–163.
58. Flory, P. J. *Principles of Polymer Chemistry*; Cornell University Press: London, 1953; Chapter 8, pp 334–336.
59. Odian, G. *Principles of Polymerization*, 3rd ed.; Wiley-Interscience: New York, 1991; Chapter 3, pp 293–296.
60. Agasandyan, V. A.; Trosman, E. A.; Bagdasar'yan, Kh. S.; Litmanovich, A. D.; Shtern, V. Ya. *Vysokomol Soyed* 1966, 8, 1580.
61. Fikenscher, H.; Herrle, K. *Mod Plast* 1945, 11, 157.
62. deGennes, P. G. *Macromolecules* 1980, 13, 1069.